Biochimica et Biophysica Acta 1858 (2016) 19–29

Contents lists available at ScienceDirect

Biochimica et Biophysica Acta

journal homepage: www.elsevier.com/locate/bbamem

Global redesign of a native β-barrel scaffold

Aaron J. Wolfe [a,b], Mohammad M. Mohammad [a], Avinash K. Thakur [a,b], Liviu Movileanu [a,b,c,*]

[a] Department of Physics, Syracuse University, 201 Physics Building, Syracuse, NY 13244-1130, USA
[b] Structural Biology, Biochemistry, and Biophysics Program, Syracuse University, 111 College Place, Syracuse, NY 13244-4100, USA
[c] The Syracuse Biomaterials Institute, Syracuse University, 121 Link Hall, Syracuse, NY 13244, USA

ARTICLE INFO

Article history:
Received 30 August 2015
Received in revised form 3 October 2015
Accepted 7 October 2015
Available online 9 October 2015

Keywords:
FhuA
Single-molecule electrophysiology
Ion channel
Spontaneous gating
Membrane protein engineering

ABSTRACT

One persistent challenge in membrane protein design is accomplishing extensive modifications of proteins without impairing their functionality. A truncation derivative of the ferric hydroxamate uptake component A (FhuA), which featured the deletion of the 160-residue cork domain and five large extracellular loops, produced the conversion of a non-conductive, monomeric, 22-stranded β-barrel protein into a large-conductance protein pore. Here, we show that this redesigned β-barrel protein tolerates an extensive alteration in the internal surface charge, encompassing 25 negative charge neutralizations. By using single-molecule electrophysiology, we noted that a commonality of various truncation FhuA protein pores was the occurrence of 33% blockades of the unitary current at very high transmembrane potentials. We determined that these current transitions were stimulated by their interaction with an external cationic polypeptide, which occurred in a fashion dependent on the surface charge of the pore interior as well as the polypeptide characteristics. This study shows promise for extensive engineering of a large monomeric β-barrel protein pore in molecular biomedical diagnosis, therapeutics, and biosensor technology.

© 2015 Elsevier B.V. All rights reserved.

1. Introduction

In many situations, global engineering of membrane proteins impairs their functionality and folding state, sometimes leading to unfolded structures [1]. One class of relatively robust membrane proteins is that of transmembrane β-barrels, which are primarily found in the outer membrane (OM) of chloroplasts, mitochondria, and Gram-negative bacteria [2]. Their stiffness is determined by the presence of a barrel scaffold consisted of anti-parallel, paired β strands. The network of many hydrogen bonds between different β strands is the basis for this unique structural robustness. This feature was at the heart of many investigations in the perpetually rich area of the engineering of β-barrel membrane proteins [3–8].

Monomeric β-barrels may be used as sensing elements, which rely upon single-molecule detection [9–12]. The main advantage of the monomeric β barrel is the ease of genetic engineering or chemical modification of single-polypeptide pores and channels, thus avoiding further complications of the purifications steps for separating the targeted engineered or modified oligomer from other byproducts of the oligomerization reaction. One challenging prerequisite for using these monomeric β-barrels in single-molecule detection is obtaining a quiet single-channel electrical signature that is freed of current gating fluctuations [13], otherwise interfering with the analyte-induced current blockades resulted from single-molecule detection. Spontaneous fluctuations in β-barrel protein channels, pores, and porins have been extensively explored [7,14–21]. In general, these fluctuations are produced by conformational alterations of the large extracellular loops, which many times permanently or transiently fold back into the pore interior [7,16].

An example of a versatile monomeric β-barrel model for extensive engineering and structure-function relationship studies is the outer membrane protein G (OmpG) from *E. coli* [22,23], a 14-stranded β-barrel containing seven extracellular loops. It was identified that the motions of loop L6 determined the gating fluctuations observed with the wild-type OmpG protein [9]. Later, other groups independently confirmed that indeed L6 is responsible for the intense gating activity of OmpG [7,24]. Recently, OmpG was successfully used for the single-molecule detection of bulky proteins by employing chemically modified flexible tethers [11,12].

In this paper, we present a detailed examination of the global engineering of ferric hydroxamate uptake component A (FhuA) [25,26], a monomeric β-barrel OM protein of *E. coli*. This 714-residue protein includes a large, 22-stranded barrel filled by an N-terminal, 160-residue cork domain located within the pore interior (Fig. 1A and B). The β strands are connected each other by 10 short β turns and 11 long extracellular loops (Supplementary Materials, Table S1, Fig. S1, Fig. S2). The internal cross-sectional surface of the barrel is elliptical with axis lengths of 26 and 39 Å, including the average length of the side chains. FhuA primarily functions as a transporter, facilitating the navigation of Fe^{3+}, complexed by the siderophore ferrichrome, from the extracellular

* Corresponding author at: Department of Physics, Syracuse University, 201 Physics Building, Syracuse, NY 13244-1130, USA.
E-mail address: lmovilea@syr.edu (L. Movileanu).
URL: http://movileanulab.syr.edu (L. Movileanu).

http://dx.doi.org/10.1016/j.bbamem.2015.10.006
0005-2736/© 2015 Elsevier B.V. All rights reserved.

into periplasmic side [27]. In addition, it was determined that FhuA functions as a transporter for antibiotics, such as albomycin [28,29] and rifamycin [30]. Remarkably, the transporter function of FhuA extends to receptor for colicin M and a number of bateriophages, including T1, T5, and ϕ80 [29].

Here, we show that deletion of the entire cork domain (ΔC) and part of five extracellular loops, L3, L4, L5, L10, and L11 (ΔL5) of FhuA results in a protein pore that is amenable to modular global engineering (Fig. 1C; Supplementary Materials, Tables S2-S4, Fig. S3). FhuA ΔC/Δ5L was further redesigned by neutralizing 25 negative charges throughout the β turns, β strands, and extracellular loops (FhuA ΔC/Δ5L-25 N; Fig. 1D). A common trait of both truncation FhuA-based protein pores was the occurrence of uniform current transitions, whose amplitude was about 33% of the unitary current, among four long-lived substates at very high positive and negative transmembrane potentials of 180 mV. Subsequent deletion of extracellular loops, encompassing part of the already deleted loops L4 and L5, as well as additional two loop deletions L7 and L8 (FhuA ΔC/Δ7L-30 N; Fig. 1E and F), produced

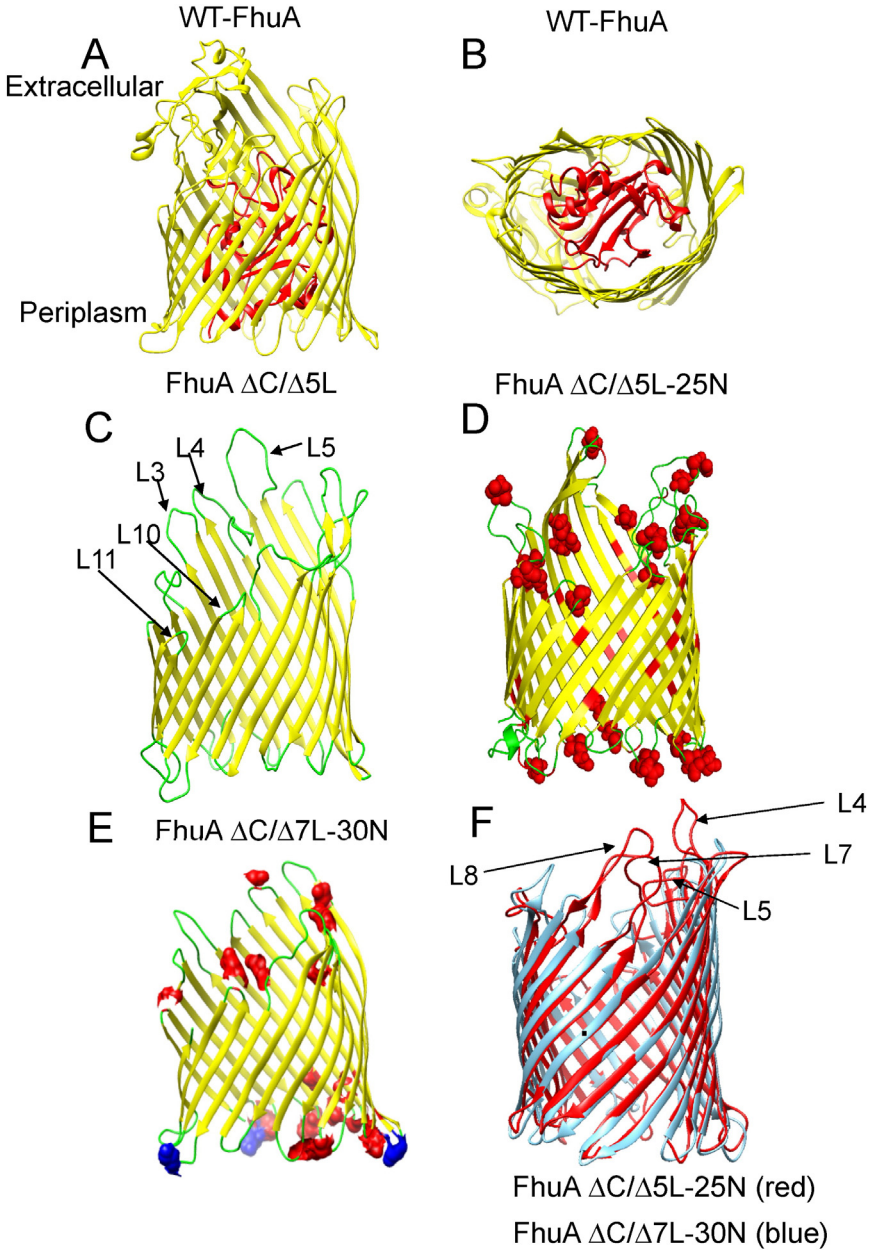

Fig. 1. Homology molecular structures created by Swiss-model [60,61] to visually compare the global mutational alterations of the β-barrel scaffold of FhuA with respect to wild-type FhuA (WT-FhuA). (A) Side view of the ribbon structure of the WT-FhuA protein [25,26]; (**B**) Top view, from the extracellular side, of the ribbon structure of the WT-FhuA protein. In (**A**) and (**B**), the 160-residue cork domain is illustrated in red; (**C**) FhuA ΔC/Δ5L encompassing complete deletion of the cork domain (ΔC) and the major deletions of five extracellular loops, L3, L4, L5, L10, and L11, which are marked by arrows; (**D**) The FhuA ΔC/Δ5L-25 N derivative highlighting the location of 25 negative charge neutralizations, marked in red, with respect to FhuA ΔC/Δ5L; (**E**) FhuA ΔC/Δ7L-30 N that has been obtained by additional four extracellular loop deletions with respect to the FhuA ΔC/Δ5L scaffold. This mutant contains 30 new positive charges with respect to FhuA ΔC/Δ5L. Additional negative charge neutralizations with respect to FhuA ΔC/Δ5L are marked in red, along with three additional lysine mutations in the β turns, out of which two are negative-to-positive charge reversals [62], which are marked in blue; (**F**) The superposition of the FhuA ΔC/Δ5L-25 N scaffold, marked in red, and FhuA ΔC/Δ7L-30 N, marked in blue, aligned and visualized by Chimera software package [63], highlighting the additional extracellular loop truncations of L4, L5, L7, and L8. All panels show the global FhuA derivatives from various angles for the sake of the clarity of specific details. Based on the X-ray crystal structure of FhuA [25,26], the average luminal dimensions of FhuA ΔC/Δ5L were determined to be ~3.1 × 4.4 nm, as measured from C_α to C_α. All homology structures of the globally mutated FhuA proteins were accomplished using FhuA PDB ID: 1FI1 [26].

a quiet electrical signature at positive potentials, but frequent, large-amplitude, and short-lived current blockades at negative potentials that were never observed with the other truncation FhuA mutants.

Interestingly, we found that the 33% current blockades observed with FhuA ΔC/Δ7L-30 N were stimulated by its interaction with a short, 23-residue cationic polypeptide at lower positive transmembrane potentials of ~120 mV. This phenomenon was also replicated with the more acidic FhuA ΔC/Δ5L protein pore interacting with other cationic polypeptides. Therefore, we concluded that not only a high transmembrane potential, but also the presence of a "polypeptide collider" within the pore interior "stimulates" the occurrence of the 33% current transitions. We postulated that not only an external polypeptide, but also an internal, fluctuating polypeptide loop activates these transitions at lower transmembrane potentials. In accord with this hypothesis, under these conditions we noted standard 33% current blockades with a redesigned β-barrel, FhuA ΔC/Δ5L-25 N_ELP, featuring an extended elastin-like-polypeptide (ELP) loop engineered within the central part of the barrel. This extensive engineering of truncated FhuA-based protein pores demonstrates their modularity, allowing for further adaptations intended for the use in medical biotechnology, therapeutics, and biosensor arenas.

2. Materials and methods

2.1. Protein overexpression and purification under denaturing condition

Details on cloning of various multi-site mutants, which were derived from Fhua Δc/Δ5 l, are provided in supplementary materials. All proteins were expressed in *E. coli* BL21 (DE3). Cells, transformed with pPR-IBA1-*fhua Δc/Δ5l-6×His*$^+$, pPR-IBA1-*fhua Δc/Δ5l-25n-6×His*$^+$, pPR-IBA1-*fhua Δc/Δ5l-25n_elp-6×His*$^+$, and pPR-IBA1-*fhua Δc/Δ7l-30n-6×His*$^+$ plasmids, were grown in *2×* TY media at 37 °C until OD600 ~0.7–0.8, at which time the protein expression was induced with 0.5 mM isopropyl β-D-1-thiogalactopyranoside (IPTG) and allowed to continue until the cell growth plateaued, as measured by OD600. Cells were harvested by centrifugation and the pellet was resuspended in the resuspension buffer (1× PBS, pH 8.0). The resuspended cells were lysed using a microfluidizer, model 110 L (Microfluidics, Newton, MA). The homogenate was centrifuged for 20 min at 4000 ×*g* and 4 °C. Inclusion bodies-containing pellets were resuspended in the inclusion body-cleaning buffer (1× PBS, 1% triton ×100, pH 8.0), homogenized using potter-Elvehjem homogenizer (VWR, Bridgeport, NJ), and recentrifuged for 30 min at 30,000 ×*g* and 4 °C. This step was repeated three times. The final pellet was resuspended in denaturing buffer (10 mM potassium phosphate, 8 M urea, pH 8.0). The solution was subject to an additional 30 min-duration centrifugation at 30,000 ×*g* and 4 °C to remove the insoluble materials. The final protein-containing solutions were filtered using 0.2 μM filters (thermo fisher scientific, Rochester, NY). The solubilized proteins were loaded onto a column packed with 2 ml of Ni +-NTA resin (Bio-Rad, Hercules, CA), which was equilibrated in 200 mM NaCl, 10 mM potassium phosphate, 8 M urea, pH 8.0. The column was washed in two steps with 5 and 25 mM imidazole, respectively, in the same equilibrating buffer. The proteins were eluted with equilibrating buffer containing 350 mM imidazole in 5 ml fractions. SDS-PAGE was used to monitor the elution profile of pure proteins

The tag-free FhuA ΔC/5 L protein, lacking the N-terminal, 33-residue signal polypeptide and the C-terminal, 6 × His$^+$ tag, named TL-FhuA ΔC/5 L, was also transformed into the *E. coli* BL21 (DE3) cells, which were grown and harvested as describe above. Cell lysates were centrifuged at 1800 ×*g* for approximately 15 min to separate the insoluble from the soluble proteins. The pellet was washed twice by resuspending it in washing buffer 1 (150 mM NaCl, 50 mM Tris, 1 mM ETDA, 2 M urea, pH 8.0) and centrifuging it for 20 min at 1800 ×*g* and 4 °C. Then, the resulting pellet was washed twice by resuspending it in washing buffer 2 (150 mM NaCl, 50 mM Tris, 1 mM EDTA, 1% Triton X-100, pH 8.0) and centrifuging it for 20 min at 1800 ×*g* and 4 °C. This procedure was followed by additional two washes of the pellet with ddH_20 and its centrifugation for 20 min at 1800 ×*g* and 4 °C. Finally, the pellet was denatured in the denaturing buffer (20 mM Tris, 6 M urea, pH 8.0) and loaded onto the ion exchange column (Bio-Rad) equilibrated with the same denaturing buffer. Protein was eluted using a linear gradient of elution buffer (20 mM Tris, 6 M urea, 1 M NaCl, pH 8.0). Collected fractions were analyzed on the SDS-PAGE gel for purity tests. Pure fractions were dialyzed against water. The final protein samples were lyophilized and stored at −80 °C.

2.2. Refolding of FhuA ΔC/Δ5L, FhuA ΔC/Δ5L-25 N, and FhuA ΔC/Δ7L-30 N

The modifications of the protocol for obtaining FhuA ΔC/Δ5L through rapid-dilution refolding has been previously described [10]. Briefly, the method of refolding for these proteins was adopted from the protocol developed by Arora and colleagues [31]. 40 μl of 6 × His$^+$-tag purified denatured protein was 50-fold diluted into a 1.5% n-Dodecyl-β-D-maltopyranoside (DDM) solution containing 200 mM NaCl, 10 mM sodium phosphate, pH 8.0. The diluted protein samples were left overnight at 23 °C to complete the refolding process of proteins. Aggregated or misfolded proteins were removed by centrifugation at 16,000 ×*g* for 15 min. Samples were stored at −80 °C in 50 μl aliquots.

2.3. Refolding of FhuA ΔC/Δ5L-25 N_ELP and TL-FhuA ΔC/Δ5L

These particular constructs did not fare well with the rapid-dilution method, so that a slow-dialysis method was employed to increase the yield and channel activity. 1 ml of urea-denatured protein FhuA ΔC/Δ5L-25 N_ELP or TL-FhuA ΔC/Δ5L at a final concentration of ~50 μM was added to cellulose dialysis tubing (Sigma, St. Louis, MO) containing 1.5% DDM. The tubing was placed in a 5-l beaker containing a buffer solution of 200 mM NaCl, 10 mM sodium phosphate, pH 8.0. The dialysis was carried out for 48 h at 4 °C changing the solution once at 24 h. The resulting protein-containing solution was spun at 16,000 ×*g* and 4 °C to remove large insoluble aggregates. To further separate the monomeric protein from potentially misfolded or aggregated species, the supernatant was applied to a Superdex 200 size-exclusion chromatography column (GE Healthcare, Piscataway, NJ) equilibrated with 0.5% DDM in 200 mM NaCl, 10 mM sodium phosphate, pH 8.0. The proteins were eluted at the flow rate of 0.25 ml/min and their elution was monitored by the absorbance at 280 nm.

2.4. Single-channel electrical recordings on planar lipid bilayers

Electrical recordings were carried out with planar bilayer lipid membranes (BLMs) [32,33]. The two sides of the chamber, *cis* and *trans* (1.5 ml each), were separated by a 25 μm-thick Teflon septum (Goodfellow Corporation, Malvern, PA). An aperture in the septum, ~80 μm in diameter, was pretreated with hexadecane (Sigma-Aldrich, St. Louis, MO), which was dissolved in highly purified pentane (Fisher HPLC grade, Fair Lawn, NJ) at a concentration of 10% (*v*/*v*). A 1,2 diphytanoyl-*sn*-glycero-phosphatidylcholine (Avanti Polar Lipids, Alabaster, AL) bilayer was formed across the aperture. For acquiring electrical recordings at single-channel resolution, the refolded engineered proteins were added to the *cis* chamber to a final concentration of ~0.1–0.3 ng/μl. Current recordings were obtained by using a patch-clamp amplifier (Axopatch 200B, Axon Instruments, Foster City, CA), which was connected to Ag/AgCl electrodes through agar bridges. The *cis* chamber was grounded, so that a positive current (upward deflection) represents positive charge moving from the *trans* to *cis* side. A Precision T3500 Tower Workstation Desktop PC (Dell Computers, Austin, TX) was equipped with a DigiData 1322A A/D converter (Axon) for data acquisition. The signal was low-pass filtered with an 8-pole Bessel filter (Model 900; Frequency Devices, Ottawa, IL) at a frequency of 10 kHz and sampled at 50 kHz, unless otherwise stated. For data acquisition and analysis, we used the pClamp9.2 and pClamp10.3 software

packages (Axon). Details on ion selectivity measurements with asymmetric buffer conditions [34,35] are provided in Supplementary experimental methods.

3. Results

3.1. Rationale for global engineering of the FhuA scaffold

A primary goal of this work was the conversion of the 714-residue, cork-filled FhuA protein into an open transmembrane pore that can maintain its functionality in a tractable mode upon global engineering (e.g. additional loop deletions, functional loop implementation, large modification of the protein surface charge). To achieve this goal, we have inspected the structural features of this protein [25,26]. The extracellular loops L3, L4, L5, L10, and L11 are large and potentially flexible due to their random-coil structure. We determined that that extensive single-channel explorations of a multiple-truncation FhuA mutant encompassing the complete removal of the cork domain (C) as well as large deletions of the five above-mentioned extracellular loops, also called FhuA ΔC/Δ5L, revealed a quiet electrical signature over a broad range of conditions, including salt concentration (20 mM–4 M), pH (2.8–11.0), and applied transmembrane potential (−160 to +160 mV) (Supplementary Materials, Table S4, Figs. S4-S7) [10]. As compared with our prior membrane protein redesign studies [5,10], here we pursued the following three distinct goals: (i) to examine the impact of an extensive alteration in the surface charge of the pore interior on its biophysical traits. For this purpose, we redesigned and created FhuA ΔC/Δ5L-25 N, which encompassed 25 neutralizations of negatively charged residues located within the β-turns, β-barrel part and extracellular loops. This truncation FhuA mutant features a much less acidic pore; (ii) to explore the effect of further truncation of the remaining large extracellular loops on the unitary conductance. In this way, we questioned whether the presence of remaining large extracellular loops contributes to the pore constriction. To accomplish this task, we redesigned and developed FhuA ΔC/Δ7L-30 N, featuring the truncation of seven extracellular loops and the implementation of 30 new positive charges. This truncation FhuA mutant included 25 neutralizations of negatively charged residues, two negative-to-positive charge reversals, and one positive charge mutation of a neutral side chain. In this way, the pore interior of FhuA ΔC/Δ7L-30 N was even less acidic than that of FhuA ΔC/Δ5L-25 N; (iii) to investigate the effect of an engineered neutral polypeptide loop within the central part of the β-barrel on the stability of the open-state current. To conduct these measurements, we created the FhuA ΔC/Δ5L-25 N_ELP protein pore, which included an elastin-like-polypeptide loop engineered within the central part of the β-barrel of the FhuA ΔC/Δ5L-25 N scaffold. In addition, we redesigned and created a control truncation mutant, TL-FhuA ΔC/Δ5L, whose polypeptide tags at the N and C termini, namely the 33-residue signal polypeptide and 6-His^+ tag, respectively, were deleted. In this way, we wanted to test whether the N- and C-terminal polypeptide tags do alter the occurrence of the 33% current blockades observed with the other truncations FhuA mutants.

3.2. Major charge neutralization of a β-barrel scaffold maintains the electrical quietness of the pore

Here, we were interested in examining whether this β-barrel scaffold of FhuA can tolerate a large alteration in the surface charge within the pore interior. Remarkably, despite numerous charge neutralizations of FhuA ΔC/Δ5L-25 N, this engineered protein pore exhibited closely similar single-channel electrical signature as compared to that of FhuA ΔC/Δ5L (Fig. 1D; Supplementary Materials, Table S5, Figs. S8–S10). This drastic change in the number of negative charges facing the pore interior produced a significant change in ionic selectivity, from a permeability ratio (P_K/P_{Cl}) of ~5.5 recorded with FhuA ΔC/Δ5L to ~0.60 observed with FhuA ΔC/Δ5L-25 N under asymmetric conditions (Supplementary Materials).

3.3. Voltage-induced gating of the engineered pores occurs in the form of uniform, 33% current transitions among four sub-states

One striking commonality between FhuA ΔC/Δ5L and FhuA ΔC/Δ5L-25 N is the display of voltage-induced current blockades at very high transmembrane potentials of 180 mV or greater and in 1 M KCl, 10 mM potassium phosphate, pH 7.4. The occurrence of fairly uniform, ~33% current blockades at highly elevated positive potentials for the two proteins is illustrated in Fig. 2A and B. They were also noted at highly elevated negative potentials (Supplementary Materials, Figs. S11-S12). In addition, such transitions occurring among the four long-lived sub-states were reversible. It should be noted that O_1 is a fully open current sub-state, reflecting the unitary conductance, whereas O_4 is a closed current sub-state, exhibiting a very small residual current in the range of 0–20 pA at a potential of +180 mV. Therefore, the O_2 and O_3 current sub-states are intermediate states connecting the fully open and closed sub-states. It is worth mentioning that all transitions only occurred among consecutive sub-states, i.e., between O_1 and O_2, between O_2 and O_3, and between O_3 and O_4. They exhibited durations in a broad time range, from tens of milliseconds to hundreds of seconds, spanning a timescale up to six orders of magnitude

One immediate question is whether the gating mechanism is impacted by the N- or C-terminus located near the periplasmic β turns of the protein (Fig. 1). This is especially reasoned by the additional polypeptides engineered at these termini. For example, FhuA ΔC/Δ5L was fused with the 33-residue signal polypeptide at the N-terminus and the 6 × His^+ tag at the C-terminus. FhuA ΔC/Δ5L-25 N had only the 6 × His^+ tag at the C-terminus. Therefore, we redesigned and constructed a FhuA ΔC/Δ5L mutant lacking both terminal polypeptides, which was named TL-FhuA ΔC/Δ5L. Interestingly, Fig. 2C demonstrates that TL-FhuA ΔC/Δ5L exhibited 33% current transitions among the four long-lived sub-states at an applied transmembrane potential of +160 mV. Such transitions were readily detectable among $O_1 \leftrightarrow O_2 \leftrightarrow O_3$ at high negative potentials (Supplementary Materials, Fig. S13). Therefore, the polypeptides engineered at the N- and C-termini were not major perturbation factors on the stability of the open-state current of the FhuA ΔC/Δ5L protein pores.

3.4. Extensive deletions of large extracellular loops impact the four sub-state dynamics of the pore at negative potential

We wondered whether the remaining parts of extracellular loops might affect the four sub-state dynamics of the engineered FhuA ΔC/Δ5L derivatives. Therefore, we designed and constructed a multiple loop deletion mutant derived from FhuA ΔC/Δ5L-25 N and characterized by further truncation of large loops L4, L5, L7, and L8, also named FhuA ΔC/Δ7L-30 N (Fig. 1E, F; Supplementary Materials, Tables S6-S8, Figs. S14-S16). Interestingly, FhuA ΔC/Δ7L-30 N exhibited a quiet single-channel electrical signature up to +120 mV (Fig. 3A). In contrast to FhuA ΔC/Δ5L and FhuA ΔC/Δ5L-25 N, FhuA ΔC/Δ7L-30 N showed a distinctive single-channel electrical signature at negative transmembrane potentials, which was decorated by frequent, large-amplitude transient current blockades (Fig. 3B). Remarkably, at −100 mV the amplitude of some of these current transitions (O_L) was greater than 50% of that of the unitary current. These experiments also reveal the asymmetry of voltage-induced current gating of FhuA ΔC/Δ7L-30 N with respect to the polarity of the applied transmembrane potential. This single-channel electrical signature consisted of small- (O_S) and large- (O_L) current amplitude blockades (n = 3; Fig. 3C). The amplitude of these current transitions was clearly distinct from those typically displayed as 33% current blockades observed with FhuA ΔC/Δ5L and FhuA ΔC/Δ5L-25 N at positive and negative transmembrane potentials

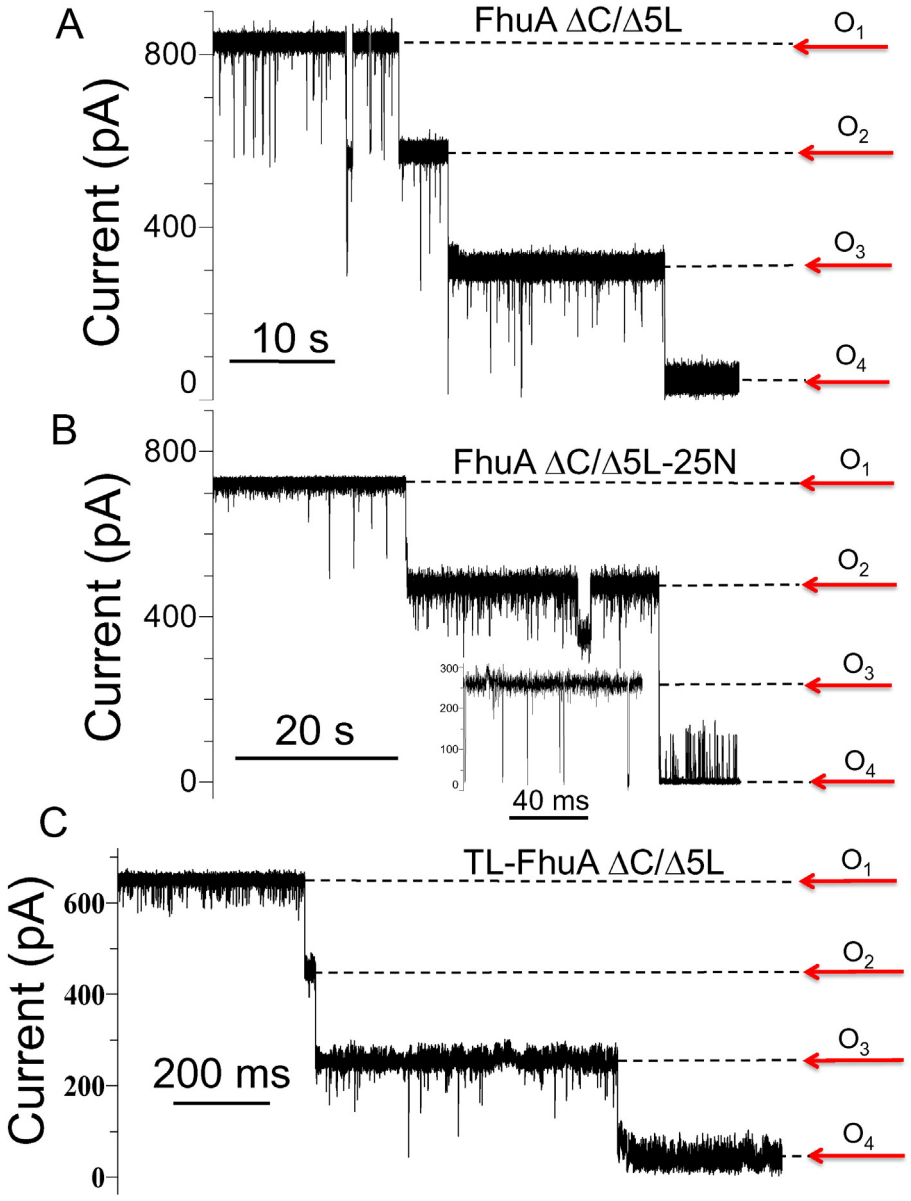

Fig. 2. Representative current blockades observed with globally mutated FhuA derivatives at very high positive potentials. These discrete blockades show each ~33% reduction in the unitary conductance. (**A**) FhuA ΔC/Δ5L at +180 mV (n = 10 distinct single-channel electrical recordings); (**B**) FhuA ΔC/Δ5L-25 N at +180 mV (n = 2). The inset shows the O_3 level by expanding the trace; (C) TL-FhuA ΔC/Δ5L at +160 mV (n = 3). All single-channel electrical recordings were achieved in 1 M KCl, 10 mM potassium phosphate, pH 7.4. Single-channel electrical traces were low-pass Bessel filtered at 1.4 kHz.

(Fig. 4). At very high negative potentials, greater than −120 mV, the FhuA ΔC/Δ7L-30 N protein pore became fairly unstable and noisy.

3.5. The 33% current transitions are stimulated by the presence of an external polypeptide collider

Remarkably, the dynamics of 33% current transitions was not only impacted by the value of applied transmembrane potential, but also by the interaction of FhuA ΔC/Δ7L-30 N with a positively charged polypeptide. Fig. 5 illustrates the interaction of Syn B2, a 23-residue polypeptide carrying five Arg residues [36] with FhuA ΔC/Δ7L-30 N at an applied potential of +120 mV. Fig. 5A shows a quiet signature of FhuA ΔC/Δ7L-30 N. When 10 μM Syn B2 was added to the *trans* side, brief transient current blockades, with dwell times $\tau_1 = 0.2$ ms and $\tau_2 = 2.45$ ms, were recorded, indicating partitioning of Syn B2 into the pore interior (Fig. 5B; Supplementary Materials, Fig. S16). No $O_2 \rightarrow O_3$ current transitions were observed under these experimental conditions (n = 3). Interestingly, increasing the Syn B2 concentration at 20 μM in the *trans* chamber determined an additional transition, $O_2 \rightarrow O_3$, and also brief Syn B2-induced current transitions reaching the O_4 sub-state (Fig. 5C).

We questioned whether this Syn B2-induced current transition between the O_2 and O_3 sub-states is only specific to its complex interactions with FhuA ΔC/Δ7L-30 N. Therefore, we executed single-channel electrical recordings with FhuA ΔC/Δ5L, which can readily undergo 33% current transitions at very high transmembrane potentials. It should be noted that a much stronger interaction between positively charged Syn B2 and the more acidic β-barrel scaffold of FhuA ΔC/Δ5L was expected, as compared to the Syn B2 - FhuA ΔC/Δ7L-30 N binding interactions. In accord with this anticipation, Syn B2 produced brief and transient current blockades at even lower transmembrane potentials (Supplementary Materials, Fig. S17). For example, in a range of transmembrane potentials between +20 and +80 mV, the dwell time of Syn B2 within the pore interior of FhuA ΔC/Δ5L was between 0.08 and 0.18 ms. A biphasic voltage dependence of the dwell time or rate

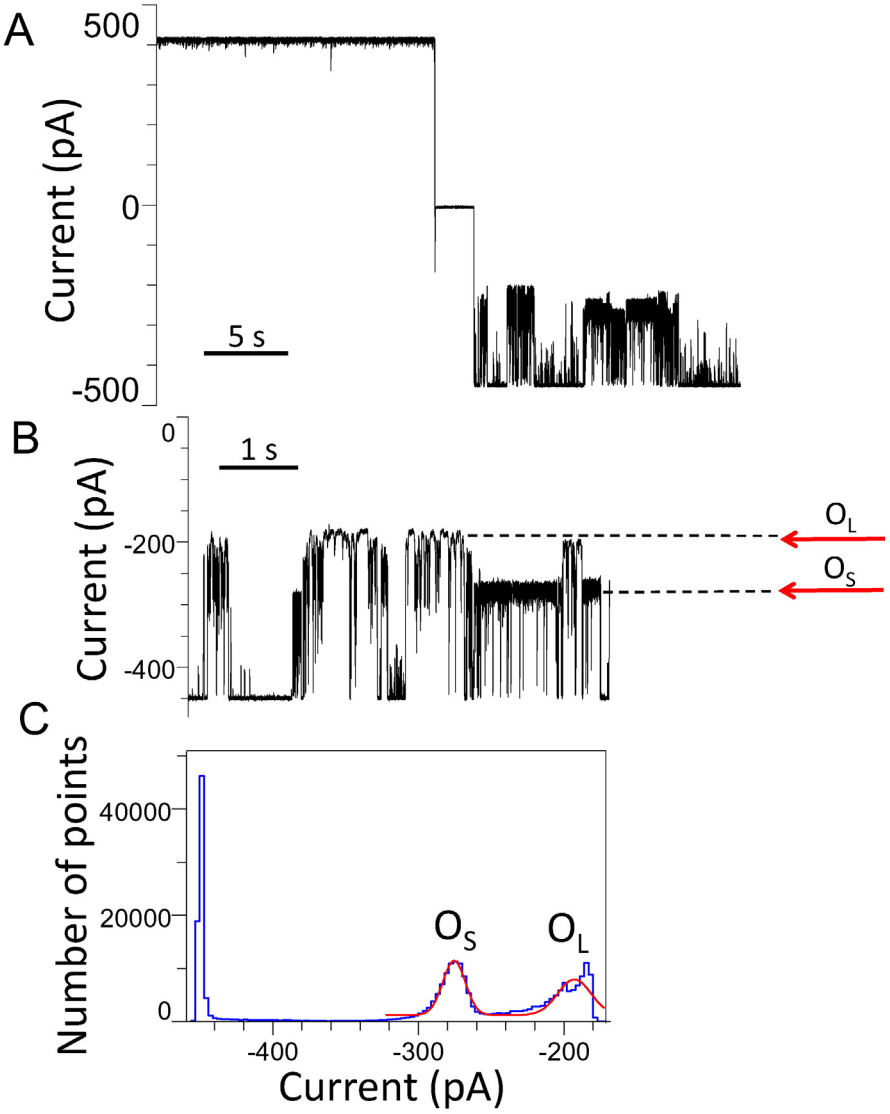

Fig. 3. Representative single-channel electrical signature of FhuA ΔC/Δ7L-30 N at a medium applied potential. (A) A representative single-channel electrical trace acquired with FhuA ΔC/Δ7L-30 N at applied transmembrane potentials of +100 and −100 mV. Transient, large-amplitude current fluctuations were observed at negative potentials; (B) a snapshot of a single-channel channel electrical recording obtained at a negative potential of −100 mV. The 33% closures were absent at either positive or negative potentials; (C) All-point current amplitude histogram of the electrical trace acquired in (B). These traces are representative over a number of at least four distinct single-channel electrical recordings. All single-channel electrical recordings were achieved in 1 M KCl, 10 mM potassium phosphate, pH 7.4. The other experimental conditions were similar to those reported in Fig. 2.

constant indirectly suggests that the relatively short Syn B2 polypeptide rapidly navigates across the pore interior of FhuA ΔC/Δ5L at potentials greater than a critical value [36–38]. The conspicuous lack of the 33% blockades might likely be determined by the rapid Syn B2 translocation.

Therefore, we examined the interaction of larger cationic polypeptides with FhuA ΔC/Δ5L, which would exhibit an even stronger binding interaction. First, we conducted single-channel recordings involving a 55-residue nucleocapsid protein 7 (NCp7) [39], a protein biomarker of the HIV-1 virus. The formal charge of NCp7 is +9 [32,40,41]. The addition of 20 μM NCp7 to the *trans* side at a transmembrane potential of only +80 mV resulted in not only frequent, transient and brief current blockades with a duration of <1 ms (n = 3), but also 33% current transitions among long-lived sub-states, such as $O_1 \rightarrow O_2$, $O_2 \rightarrow O_3$, and $O_3 \rightarrow O_4$ (Supplementary Materials, Fig. S18). It is worth noting that the amplitude of the brief transient current blockades was closely similar to the 33% normalized amplitude of the current transitions between the above-mentioned sub-states. Similarly with that situation of the interactions between Syn B2 and FhuA ΔC/Δ7L-30 N, we found that the probability of the NCp7-induced 33% current transitions in FhuA ΔC/Δ5L was strongly dependent on the concentration of the external polypeptide. For example, at +80 mV, the first $O_1 \rightarrow O_2$ transition occurred after a period of 253 ± 1 s (n = 2), 103 ± 2 s (n = 3), and 9 ± 13 s (n = 5) when 200 nM, 5 μM, and 20 μM were added to the *trans* chamber, respectively.

Moreover, we also inspected the interaction of the much larger pb_2-Ba proteins [42] with FhuA ΔC/Δ5L. pb_2-Ba consists of the N terminal region of the pre-cytochrome b_2 (pb_2) of varying length (indicated as number of residues in parenthesis) fused to the N-terminus of the small ribonuclease barnase (Ba). They feature a high positive charge located on the leading sequence pb_2 [36]. Under experimental conditions similar to those involving NCp7, we were able to detect the 33% current blockades $O_1 \rightarrow O_2$, $O_2 \rightarrow O_3$, and $O_3 \rightarrow O_4$ at a transmembrane potential of +80 mV when only 200 nM of pb_2-Ba was added to the *trans* side (Supplementary Materials, Fig. S18).

3.6. The 33% current transitions are stimulated by the presence of an engineered polypeptide loop within the pore interior

Based on findings pertinent to the impact of an external polypeptide collider on the dynamics of the 33% current transitions in FhuA ΔC/Δ5L and FhuA ΔC/Δ7L-30 N protein pores, we hypothesized that discrete 33%

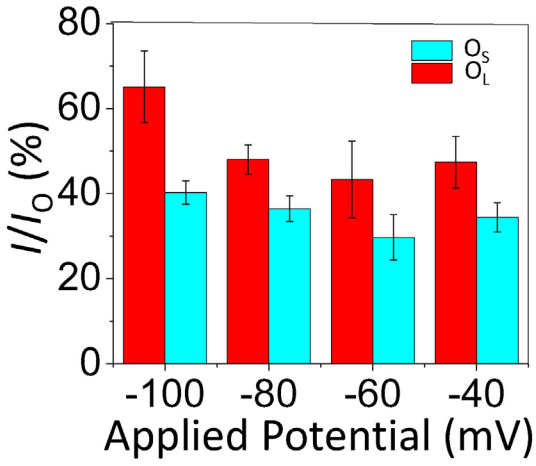

Fig. 4. FhuA ΔC/Δ7L-30 N shows a distinctive signature from the other truncation FhuA mutants. Current-amplitude histogram of the highly frequent current blockades observed with FhuA ΔC/Δ7L-30 N at negative potentials. The current amplitudes were normalized to that value corresponding to the unitary current. All single-channel electrical recordings were achieved in 1 M KCl, 10 mM potassium phosphate, pH 7.4. The other experimental conditions were similar to those reported in Fig. 2.

current transitions among long-lived "metastable" sub-states can also be stimulated by the presence of an endogenously engineered polypeptide within the pore interior. Therefore, we engineered an elastin-like-polypeptide (ELP) loop by replacing Arg115 in the 6th β-strand, which is near the central part of the native β-barrel scaffold. The sequence of the ELP was $(VPGGG)_{10}$, and was supplemented by two flexible Gly-Ser-based linkers, thus totaling 65 residues for the entire engineered polypeptide. The newly made construct, named FhuA ΔC/Δ5L-25 N_ELP, was extensively examined under similar conditions with the other truncation FhuA mutants. This polypeptide lacks charge, avoiding some strong electrostatic interactions with the barrel walls. In addition, ELP is expected to be in expanded conformation [43,44], perhaps reaching the extracellular region of the pore. In excellent accord with our above-mentioned postulation, Fig. 6A presents typical 33% current blockades of FhuA ΔC/Δ5L-25 N_ELP occurring among all four long-lived sub-states at an applied transmembrane potential of −100 mV, a condition at which we have never noted such events with the FhuA ΔC/Δ5L-25 N protein alone or with other truncation FhuA mutant. These 33% current transitions among long-lived sub-states were fully reversible (Fig. 6B; Supplementary Materials, Fig. S19).

3.7. Conserved single-channel signatures of the globally engineered FhuA protein pores

In this work, all globally mutated FhuA protein pores showed 33% current transitions, except FhuA ΔC/Δ7L-30 N at negative transmembrane potentials. Another conserved property of these proteins is their close similarity in unitary conductance. In Fig. 7A, the current–voltage plot illustrates an almost linear profile with little deviations in single-channel current. Interestingly, although the probability of occurrence of discrete current transitions among the four long-lived sub-states depended on various factors, including the applied transmembrane potential, the concentration of the external polypeptide collider or the presence of an internally fluctuating polypeptide, their conductance amplitude, ~1.3 nS, was independent of the applied transmembrane potential (Fig. 7B). This finding suggests that these particular transitions observed with all explored globally engineered FhuA protein pores are produced by the same gating mechanism.

4. Discussion

In this work, we extensively investigated truncation FhuA mutants lacking the cork domain and significant parts of several large extracellular loops. The large negative charge neutralization demonstrated the ability to modulate ion selectivity of a 22-stranded β-barrel protein in a predictive manner, from a strongly cation-selective to a weakly anion-selective pore. More importantly, this ion selectivity change was accomplished without a significant perturbation of primary biophysical traits, such as the unitary conductance of the protein pore, the quietness of its single-channel electrical signature under a broad range of experimental conditions, as well as the occurrence of the symmetrical 33% current blockades at very high transmembrane potentials.

The amplitudes of these 33% current blockades were not voltage dependent. Their occurrence was symmetric with respect to the polarity of the applied voltage, except those noted with FhuA ΔC/Δ7L-30 N. Ample changes in extracellular loops encompassing additional five positive charges perturbed the energetic landscape of the protein pore at negative potentials. The $O_1 \rightarrow O_2$ transitions were still detectable with FhuA ΔC/Δ7L-30 N at lower positive potentials than those observed with FhuA ΔC/Δ5L-25 N, indicating that this gating mechanism is independent of the absence of large extracellular loops L3, L4, L5, L7, L8, L10, and L11. These current transitions were independent of the protein alterations at the N and C termini, as demonstrated with a TL-FhuA truncation mutant, as well as extensive charge modifications within the pore interior and major deletions of the extracellular loops. We speculate that these current transitions resulted from potential breathing deformations of the overall architecture of the β-barrel embedded into the bilayer, such as stretching and compression. The phenomenon of breathing fluctuations [45,46] underlying the gating process was recently proposed in the case of outer membrane protein G (OmpG) of *Escherichia coli*, a monomeric, 14-stranded β-barrel [7] and voltage-dependent anion channel (VDAC) [46]. Interestingly, Geng and colleagues reported voltage-induced 33% gating blockades among long-lived sub-states occurring in the phi29 connector protein channel [47]. A lack of crystallographic data of these truncation FhuA mutants precluded the obtaining of the molecular origin of the 3-fold nature of these current transitions among the four long-lived sub-states. One possibility would be that the surface molecular charge distribution throughout the pore interior features an almost 3-fold symmetry, so these current transitions in a 3-fold fashion are governed by strong electrostatic forces that span across the inner surface of the β barrel. We extensively examined the residue charge distribution within the β turns, β barrel, and undeleted extracellular loops and found a heterogeneous charge density throughout these regions of the protein, but without a 3-fold symmetry (Supplementary Materials, Fig. S20). The fact that FhuA ΔC/Δ5L_25N, which is characterized by 25 neutralizations of negative charges within the pore interior, underwent 33% current blockades in a closely similar fashion with FhuA ΔC/Δ5L, strongly indicates that the charge density and distribution of β barrel is not a key player in such current transitions. It is also true that flexibility of the barrel depends on other factors, such as the hydrophobic interactions with the phospholipids of the bilayer as well as the side chains of the hydrophilic residues facing the pore interior. Therefore, it is unclear what are the dominant forces driving the pore structure in a "sub-trimeric" conformation.

It is conceivable that the duration of these "metastable" sub-states is modulated by transient pushing-pulling forces on the barrel wall. For example, an external polypeptide collider partitioning within the pore interior perturbed the system by transiently pushing the pore walls. In contrast, an engineered polypeptide loop within the β barrel acted as an elastic spring pulling the walls through its conformational fluctuations [48]. At very high transmembrane potentials of ~180 mV, these pushing-puling forces are amplified by the thickness, bending and stretching fluctuations of the lipid bilayer [49,50].

To our knowledge, these extensive truncations and global modifications of FhuA are the largest ever of a 22-stranded β-barrel examined by single-channel electrical recordings. In contrast to large-truncation FhuA protein pores encompassing several loop deletions as well as cork removal, shorter deletion mutants of FhuA exhibited complex voltage-induced current gating even at low applied transmembrane

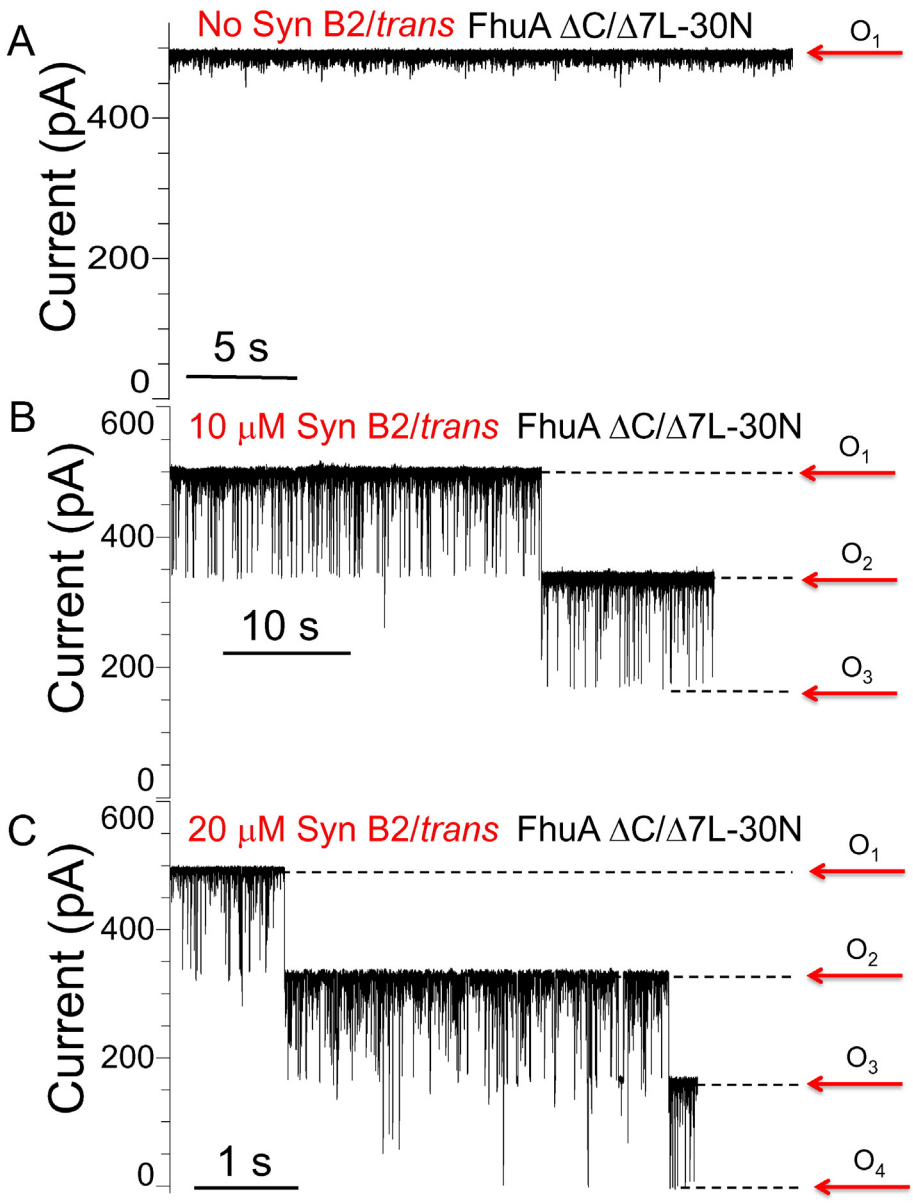

Fig. 5. Discrete current blockades observed with FhuA ΔC/Δ7L-30 N in the presence of Syn B2. (**A**) A representative single-channel electrical trace acquired with FhuA ΔC/Δ7L-30 N; (**B**) Application of low concentrations of the Syn B2 polypeptide to the *trans* side caused a 33% current blockade; (**C**) Application of increased concentrations of the Syn B2 polypeptide produced an additional 33% current blockade over that noted with FhuA ΔC/Δ7L-30 N alone. All single-channel electrical recordings were accomplished at an applied potential of +120 mV. All single-channel electrical recordings were achieved in 1 M KCl, 10 mM potassium phosphate, pH 7.4. The other experimental conditions were similar to those reported in Fig. 2.

potentials. For example, the truncation of the cork domain resulted in highly noisy FhuA ΔC single-channels [5,51], which included frequent openings to a ~ 2.5-nS conductance state. Interestingly, a truncation mutant of FhuA that featured the deletion of the cork domain, gating loop L4 and strand β7, showed a uniform 3.2-nS conductance open state decorated by brief 33% current blockades [5]. Currently, it is not clear whether these brief current transitions are generated by the same gating mechanism driving the 33% current blockades in the case of large-truncation FhuA pores.

Surprisingly, the ELP loop-containing FhuA ΔC/Δ5L-25 N showed insignificant change in the unitary conductance, but a voltage-induced gating activity at transmembrane potentials at which 33% current blockades were never observed in either FhuA ΔC/Δ5L or FhuA ΔC/Δ5L-25 N. These experiments also demonstrate the opportunity for engineering a functional polypeptide plug at a different location than that in FhuA ΔC/Δ5L-25 N_ELP. Therefore, we postulate that there is no technical difficulty in permanent placing other stimuli-responsive polypeptides plugs [52] in various locations, such as the N and C termini as well as within the extracellular side of the protein. That would create of new class of proteinaceous nanodevices for controlling the transport of various compounds through lipid membranes of capsules as a result of a change in an environmental, physical or chemical parameter, such as temperature, pH, local osmotic gradient, redox potential, or light.

The relatively large size of the barrel, encompassing 22 anti-parallel β strands, provides prospects for the creation of protein nanovalves with relatively bulky polypeptide occlusions featuring different architectures [53]. If these developments would be coupled with extensive alterations of the surface charge of the β barrel, whose feasibility is demonstrated in this work, then such a generic protein nanovalve with controllable occlusions might be used in a broad range of arenas in medical biotechnology and therapeutics. As a matter of fact, not only FhuA [27,54,55], but also other outer membrane proteins, such as the PapC usher, a dimeric 24-stranded β-barrel of *E. coli* [15,20,56,57], has a gating cork domain that undergoes conformational transitions upon an external chemical stimulus. Thus, the functionality of globally engineered FhuA-based protein pores would rely on a closely related

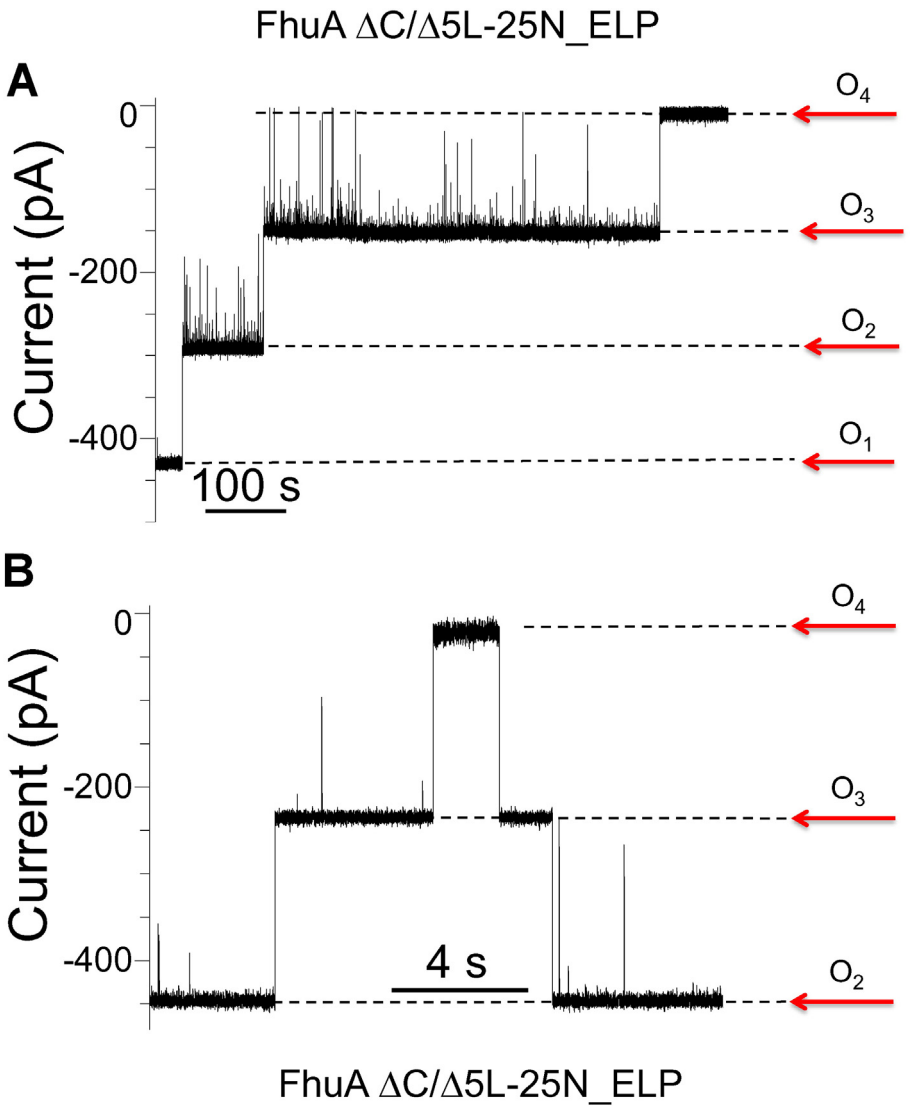

Fig. 6. Representative 33% current blockades observed with FhuA ΔC/Δ5L-25 N_ELP. (**A**) The transmembrane potential was −100 mV; (**B**) A short section of a typical single-channel electrical trace showing that the 33% current transitions observed with FhuA ΔC/Δ5L-N25_ELP were reversible. The transmembrane potential was −155 mV. These electrical traces are representative over a number of seven independent experiments. All single-channel electrical recordings were achieved in 1 M KCl, 10 mM potassium phosphate, pH 7.4. The other experimental conditions were similar to those reported in Fig. 2.

mechanism inspired by those existent in nature. Overall, with β-barrel adaptations and further development, such engineered polypeptide plugs can be explored as a controllable delivery mechanism.

The 33% current transitions were also observed by interactions of cationic polypeptides with the interior of the globally engineered FhuA proteins when added to the *trans* side of the chamber. The frequency of these transitions was certainly dependent not only on the nature of the polypeptide, such as its length and charge, but also its concentration. If we take into account the dimensions of the elliptical β barrel of FhuA excluding the cork domain, but including the side chains of the residues, such as the axis lengths $a = 26$ Å and $b = 39$ Å, as well as a minimum height, $h_{min} = 20$ Å, and a maximum height, $h_{max} = 40$ Å, then the calculated volume would have a value between 16,000 and 32,000 Å^3. The molecular weight of the engineered ELP loop, including the flexible Gly-Ser linkers was 4.8 kDa. The effective concentration within the pore interior is $[ELP] = 1/(N_A V_{barrel})$ [58], where N_A is Avogadro's number and V_{barrel} is the internal volume of the β barrel. Under these conditions, the effective ELP concentration within the β barrel would be between 5.3 and 10.6 mM. This ELP concentration level is ~267 and ~533 times greater than the free concentration of Syn B2 producing the $O_2 \rightarrow O_3$ transition in FhuA ΔC/Δ7L-30 N, respectively. The fact that these current transitions also occurred within FhuA ΔC/Δ5L-25 N_ELP at lower applied potentials, indicated that the cationic nature of the interacting polypeptide was just a requirement for its electrophoretic capture into the pore interior. This finding is consistent with a charge-independent pushing-pulling mechanism on the pore walls, as postulated above.

Given the observed long-lived sub-states, O_1, O_2, O_3, and O_4, it is difficult to infer the quantitative nature of the activation free energies for the transitions from one sub-state to another. For events lasting tens of seconds or minutes, the acquisition time of such single-channel electrical recordings would have to be in the order of several days. One possibility to address this challenge is to conduct these experiments at elevated temperatures [17,59]. In this way, the activation free energies will decrease, shortening the duration of the time constants that correspond to all sub-states. This approach will reveal the most frequent transitions as well as the enthalpic and entropic contributions to all transition-rate constants governing these globally engineered FhuA protein pores [33]. Drastic architectural modifications in the form of extensive deletions of extracellular loops and major modulation of the surface charge resulted in insignificant alterations of the single-channel conductance of these globally engineered FhuA protein pores,

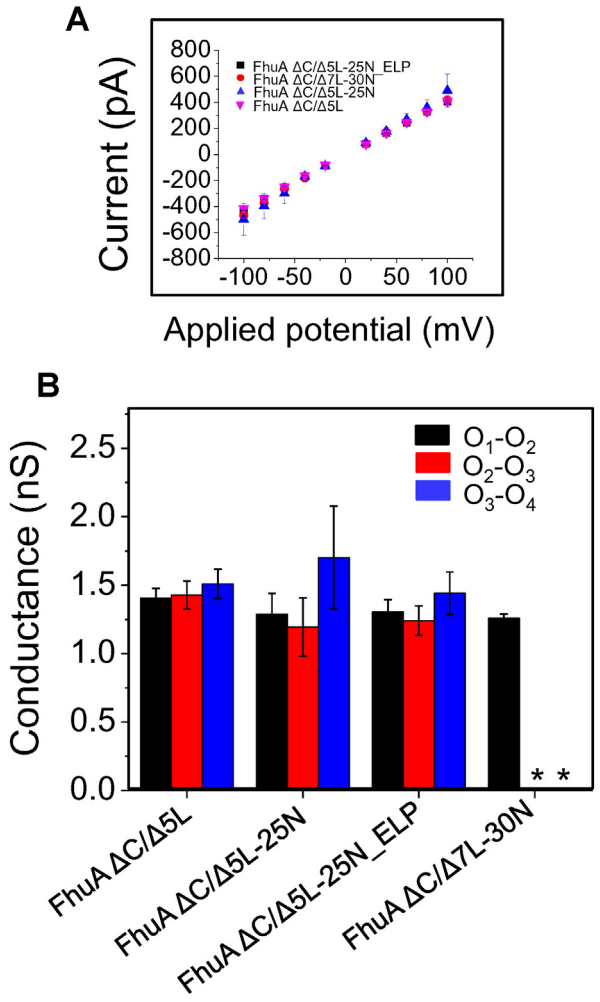

Fig. 7. Conserved single-channel features of the truncation FhuA mutants. (**A**) The current–voltage relationship represented as average ± SD over at least three independent experimental determinations; (**B**) Voltage-induced current blockades with a normalized current amplitude of 33% are ubiquitous among all globally mutated FhuA proteins. Data represent normalized amplitude of the conductance of the current blockades from one discrete open sub-state to the other with respect to open sub-state (O_1) unitary conductance. All current blockades were ~1.3 nS in conductance or ~33% of the open sub-state (O_1) unitary conductance. "*" stand for unavailable data, because we were not able to note such transitions in FhuA ΔC/7 L-30 N alone. All single-channel electrical recordings were achieved in 1 M KCl, 10 mM potassium phosphate, pH 7.4. The other experimental conditions were similar to those reported in Fig. 2.

suggesting tractability and modularity features of this β-barrel scaffold, and in turn the feasibility to utilize this large redesigned protein pore in a wide range of applications. These characteristics will allow in the future obtaining conclusive and informative data pertinent to the perturbations of this β-barrel protein system. An absence of a significant change in the unitary conductance following extensive deletions in the extracellular loops implies that the constriction of these mutants does not seem to be created by the large extracellular loops folding back into the pore interior.

In summary, we demonstrated the versatility of the native β-barrel scaffold of FhuA to global engineering, showing modularity to β turn, β barrel and extracellular loop engineering. New aspects of this work included the extensive truncation of a large, 22-stranded β barrel up to seven extracellular loops, drastic alteration in the surface negative charge neutralization, up to 30 new positive charges, and engineering of a neutral polypeptide loop within the pore interior. Heavily redesigned FhuA ΔC/Δ7L-30 N exhibited a great disparity of the single-channel electrical signature between positive and negative transmembrane potentials. In this case, brief current blockades noted at negative potentials do not seem to fit within the confines of the gating mechanism responsible for 33% current fluctuations between the fourth long-lived and discrete current sub-states. With further development of such a truncation FhuA-based mutant, one can design and create a polarity-induced molecular switch, in which the redesigned FhuA protein is fully conductive at a positive potential, but closed at a negative potential. This study represents a platform for future extensive engineering of FhuA for targeted applications in therapeutics and molecular biomedical technology.

Conflict of interest

The authors declare no competing financial interest.

Author contribution

A.J.W. designed research, performed experiments, conducted data analysis, and wrote the paper; M.M.M. designed research, performed experiments, and conducted data analysis; A.K.T. designed research, performed experiments, and conducted data analysis; L.M. designed research and wrote the paper.

Acknowledgments

The authors thank Noriko Tomita, Manu K. Arul, Jeffrey R. Roberge and Josh Mills for their technical assistance during the early stage of this subproject. We are grateful to Khalil R. Howard for the redesign of FhuA ΔC/Δ5L-25 N and Phil Borer for the NCp7 polypeptide. This work was supported by the National Institutes of Health grant R01 GM088403 (to L.M.).

Appendix A. Supplementary Data

Supplementary data to this article can be found online at http://dx.doi.org/10.1016/j.bbamem.2015.10.006.

References

[1] K.G. Fleming, Energetics of membrane protein folding, Annu. Rev. Biophys. 43 (2014) 233–255.
[2] W.C. Wimley, The versatile beta-barrel membrane protein, Curr. Opin. Struct. Biol. 13 (2003) 404–411.
[3] H. Bayley, L. Jayasinghe, Functional engineered channels and pores (review), Mol. Membr. Biol. 21 (2004) 209–220.
[4] H. Hong, G. Szabo, L.K. Tamm, Electrostatic couplings in OmpA ion-channel gating suggest a mechanism for pore opening, Nat. Chem. Biol. 2 (2006) 627–635.
[5] M.M. Mohammad, K.R. Howard, L. Movileanu, Redesign of a plugged beta-barrel membrane protein, J. Biol. Chem. 286 (2011) 8000–8013.
[6] M. Pavlenok, I.M. Derrington, J.H. Gundlach, M. Niederweis, MspA nanopores from subunit dimers, PLoS One 7 (2012), e38726.
[7] W. Grosse, G. Psakis, B. Mertins, P. Reiss, D. Windisch, F. Brademann, J. Burck, A.S. Ulrich, U. Koert, L.O. Essen, Structure-based engineering of a minimal porin reveals loop-independent channel closure, Biochemistry 53 (2014) 4826–4838.
[8] D. Stoddart, M. Ayub, L. Hofler, P. Raychaudhuri, J.W. Klingelhoefer, G. Maglia, A. Heron, H. Bayley, Functional truncated membrane pores, Proc. Natl. Acad. Sci. U. S. A. 111 (2014) 2425–2430.
[9] M. Chen, S. Khalid, M.S. Sansom, H. Bayley, Outer membrane protein G: engineering a quiet pore for biosensing, Proc. Natl. Acad. Sci. U. S. A. 105 (2008) 6272–6277.
[10] M.M. Mohammad, R. Iyer, K.R. Howard, M.P. McPike, P.N. Borer, L. Movileanu, Engineering a rigid protein tunnel for biomolecular detection, J. Am. Chem. Soc. 134 (2012) 9521–9531.
[11] M. Fahie, C. Chisholm, M. Chen, Resolved single-molecule detection of individual species within a mixture of anti-biotin antibodies using an engineered monomeric nanopore, ACS Nano 9 (2015) 1089–1098.
[12] M.A. Fahie, M. Chen, Electrostatic interactions between OmpG nanopore and analyte protein surface can distinguish between glycosylated isoforms, J. Phys. Chem. B 119 (2015) 10198–10206.
[13] B. Sackmann, E. Neher, Single-Channel Recording, Second edition Kluwer Academic/Plenum Publishers, New York, 1995.
[14] L. Kullman, P.A. Gurnev, M. Winterhalter, S.M. Bezrukov, Functional subconformations in protein folding: evidence from single-channel experiments, Phys. Rev. Lett. 96 (2006) 038101.
[15] O.S. Mapingire, N.S. Henderson, G. Duret, D.G. Thanassi, A.H. Delcour, Modulating effects of the plug, helix, and N- and C-terminal domains on channel properties of the PapC usher, J. Biol. Chem. 284 (2009) 36324–36333.

[16] B.R. Cheneke, B. van den Berg, L. Movileanu, Analysis of gating transitions among the three major open states of the OpdK channel, Biochemistry 50 (2011) 4987–4997.
[17] B.R. Cheneke, M. Indic, B. van den Berg, L. Movileanu, An outer membrane protein undergoes enthalpy- and entropy-driven transitions, Biochemistry 51 (2012) 5348–5358.
[18] E. Eren, J. Vijayaraghavan, J. Liu, B.R. Cheneke, D.S. Touw, B.W. Lepore, M. Indic, L. Movileanu, B. van den Berg, Substrate specificity within a family of outer membrane carboxylate channels, PLoS Biol. 10 (2012), e1001242.
[19] E. Eren, J. Parkin, A. Adelanwa, B.R. Cheneke, L. Movileanu, S. Khalid, B. van den Berg, Towards understanding the outer membrane uptake of small molecules by *Pseudomonas aeruginosa*, J. Biol. Chem. 288 (2013) 12042–12053.
[20] E. Volkan, V. Kalas, J.S. Pinkner, K.W. Dodson, N.S. Henderson, T. Pham, G. Waksman, A.H. Delcour, D.G. Thanassi, S.J. Hultgren, Molecular basis of usher pore gating in Escherichia coli pilus biogenesis, Proc. Natl. Acad. Sci. U. S. A. 110 (2013) 20741–20746.
[21] K.R. Pothula, U. Kleinekathofer, Theoretical analysis of ion conductance and gating transitions in the OpdK (OccK1) channel, Analyst 140 (2015) 4855–4864.
[22] O. Yildiz, K.R. Vinothkumar, P. Goswami, W. Kuhlbrandt, Structure of the monomeric outer-membrane porin OmpG in the open and closed conformation, EMBO J. 25 (2006) 3702–3713.
[23] G.V. Subbarao, B. van den Berg, Crystal structure of the monomeric porin OmpG, J. Mol. Biol. 360 (2006) 750–759.
[24] T. Zhuang, L.K. Tamm, Control of the conductance of engineered protein nanopores through concerted loop motions, Angew. Chem. Int. Ed. Engl. 53 (2014) 5897–5902.
[25] K.P. Locher, B. Rees, R. Koebnik, A. Mitschler, L. Moulinier, J.P. Rosenbusch, D. Moras, Transmembrane signaling across the ligand-gated FhuA receptor: crystal structures of free and ferrichrome-bound states reveal allosteric changes, Cell 95 (1998) 771–778.
[26] A.D. Ferguson, E. Hofmann, J.W. Coulton, K. Diederichs, W. Welte, Siderophore-mediated iron transport: crystal structure of FhuA with bound lipopolysaccharide, Science 282 (1998) 2215–2220.
[27] P.D. Pawelek, N. Croteau, C. Ng-Thow-Hing, C.M. Khursigara, N. Moiseeva, M. Allaire, J.W. Coulton, Structure of TonB in complex with FhuA, E. coli outer membrane receptor, Science 312 (2006) 1399–1402.
[28] A.D. Ferguson, V. Braun, H.P. Fiedler, J.W. Coulton, K. Diederichs, W. Welte, Crystal structure of the antibiotic albomycin in complex with the outer membrane transporter FhuA, Protein Sci. 9 (2000) 956–963.
[29] V. Braun, FhuA (TonA), the career of a protein, J. Bacteriol. 191 (2009) 3431–3436.
[30] A.D. Ferguson, J. Kodding, G. Walker, C. Bos, J.W. Coulton, K. Diederichs, V. Braun, W. Welte, Active transport of an antibiotic rifamycin derivative by the outer-membrane protein FhuA, Structure 9 (2001) 707–716.
[31] A. Arora, D. Rinehart, G. Szabo, L.K. Tamm, Refolded outer membrane protein a of Escherichia coli forms ion channels with two conductance states in planar lipid bilayers, J. Biol. Chem. 275 (2000) 1594–1600.
[32] D.J. Niedzwiecki, R. Iyer, P.N. Borer, L. Movileanu, Sampling a biomarker of the human immunodeficiency virus across a synthetic nanopore, ACS Nano 7 (2013) 3341–3350.
[33] B.R. Cheneke, B. van den Berg, L. Movileanu, Quasithermodynamic contributions to the fluctuations of a protein nanopore, ACS Chem. Biol. 10 (2015) 784–794.
[34] J. Liu, E. Eren, J. Vijayaraghavan, B.R. Cheneke, M. Indic, B. van den Berg, L. Movileanu, OccK channels from Pseudomonas aeruginosa exhibit diverse single-channel electrical signatures, but conserved anion selectivity, Biochemistry 51 (2012) 2319–2330.
[35] J. Liu, A.J. Wolfe, E. Eren, J. Vijayaraghavan, M. Indic, B. van den Berg, L. Movileanu, Cation selectivity is a conserved feature in the OccD subfamily of Pseudomonas aeruginosa, Biochim. Biophys. Acta Biomembr. 1818 (2012) 2908–2916.
[36] M.M. Mohammad, S. Prakash, A. Matouschek, L. Movileanu, Controlling a single protein in a nanopore through electrostatic traps, J. Am. Chem. Soc. 130 (2008) 4081–4088.
[37] A.J. Wolfe, M.M. Mohammad, S. Cheley, H. Bayley, L. Movileanu, Catalyzing the translocation of polypeptides through attractive interactions, J. Am. Chem. Soc. 129 (2007) 14034–14041.
[38] R. Bikwemu, A.J. Wolfe, X. Xing, L. Movileanu, Facilitated translocation of polypeptides through a single nanopore, J. Phys. Condens. Matter 22 (2010) 454117.
[39] R.N. De Guzman, Z.R. Wu, C.C. Stalling, L. Pappalardo, P.N. Borer, M.F. Summers, Structure of the HIV-1 nucleocapsid protein bound to the SL3 psi-RNA recognition element, Science 279 (1998) 384–388.
[40] A.C. Paoletti, M.F. Shubsda, B.S. Hudson, P.N. Borer, Affinities of the nucleocapsid protein for variants of SL3 RNA in HIV-1, Biochemistry 41 (2002) 15423–15428.
[41] M.F. Shubsda, A.C. Paoletti, B.S. Hudson, P.N. Borer, Affinities of packaging domain loops in HIV-1 RNA for the nucleocapsid protein, Biochemistry 41 (2002) 5276–5282.
[42] S. Huang, K.S. Ratliff, A. Matouschek, Protein unfolding by the mitochondrial membrane potential, Nat. Struct. Biol. 9 (2002) 301–307.
[43] B. Li, D.O.V. Alonso, B.J. Bennion, V. Daggett, Hydrophobic hydration is an important source of elasticity in elastin-based biopolymers, J. Am. Chem. Soc. 123 (2001) 11991–11998.
[44] B. Li, D.O.V. Alonso, V. Daggett, The molecular basis for the inverse temperature transition of elastin, J. Mol. Biol. 305 (2001) 581–592.
[45] S. Villinger, R. Briones, K. Giller, U. Zachariae, A. Lange, B.L. de Groot, C. Griesinger, S. Becker, M. Zweckstetter, Functional dynamics in the voltage-dependent anion channel, Proc. Natl. Acad. Sci. U. S. A. 107 (2010) 22546–22551.
[46] U. Zachariae, R. Schneider, R. Briones, Z. Gattin, J.P. Demers, K. Giller, E. Maier, M. Zweckstetter, C. Griesinger, S. Becker, R. Benz, B.L. de Groot, A. Lange, beta-Barrel mobility underlies closure of the voltage-dependent anion channel, Structure. 20 (2012) 1540–1549.
[47] J. Geng, H. Fang, F. Haque, L. Zhang, P. Guo, Three reversible and controllable discrete steps of channel gating of a viral DNA packaging motor, Biomaterials 32 (2011) 8234–8242.
[48] O.V. Krasilnikov, C.G. Rodrigues, S.M. Bezrukov, Single polymer molecules in a protein nanopore in the limit of a strong polymer-pore attraction, Phys. Rev. Lett. 97 (2006) 018301.
[49] L. Movileanu, D. Popescu, S. Ion, A.I. Popescu, Transbilayer pores induced by thickness fluctuations, Bull. Math. Biol. 68 (2006) 1231–1255.
[50] A.C. Woodka, P.D. Butler, L. Porcar, B. Farago, M. Nagao, Lipid bilayers and membrane dynamics: insight into thickness fluctuations, Phys. Rev. Lett. 109 (2012) 058102.
[51] M. Braun, H. Killmann, E. Maier, R. Benz, V. Braun, Diffusion through channel derivatives of the Escherichia coli FhuA transport protein, Eur. J. Biochem. 269 (2002) 4948–4959.
[52] Y. Jung, H. Bayley, L. Movileanu, Temperature-responsive protein pores, J. Am. Chem. Soc. 128 (2006) 15332–15340.
[53] L.M. Yang, P. Blount, Manipulating the permeation of charged compounds through the MscL nanovalve, FASEB J. 25 (2011) 428–434.
[54] E. Udho, K.S. Jakes, S.K. Buchanan, K.J. James, X. Jiang, P.E. Klebba, A. Finkelstein, Reconstitution of bacterial outer membrane TonB-dependent transporters in planar lipid bilayer membranes, Proc. Natl. Acad. Sci. U. S. A. 106 (2009) 21990–21995.
[55] J. Thoma, P. Bosshart, M. Pfreundschuh, D.J. Muller, Out but not in: the large transmembrane beta-barrel protein FhuA unfolds but cannot refold via beta-hairpins, Structure 20 (2012) 2185–2190.
[56] Y. Huang, B.S. Smith, L.X. Chen, R.H. Baxter, J. Deisenhofer, Insights into pilus assembly and secretion from the structure and functional characterization of usher PapC, Proc. Natl. Acad. Sci. U. S. A. 106 (2009) 7403–7407.
[57] E. Volkan, B.A. Ford, J.S. Pinkner, K.W. Dodson, N.S. Henderson, D.G. Thanassi, G. Waksman, S.J. Hultgren, Domain activities of PapC usher reveal the mechanism of action of an Escherichia coli molecular machine, Proc. Natl. Acad. Sci. U. S. A. 109 (2012) 9563–9568.
[58] L. Movileanu, S. Cheley, H. Bayley, Partitioning of individual flexible polymers into a nanoscopic protein pore, Biophys. J. 85 (2003) 897–910.
[59] C. Chimerel, L. Movileanu, S. Pezeshki, M. Winterhalter, U. Kleinekathofer, Transport at the nanoscale: temperature dependence of ion conductance, Eur. Biophys. J. 38 (2008) 121–125.
[60] N. Guex, M.C. Peitsch, T. Schwede, Automated comparative protein structure modeling with SWISS-MODEL and Swiss-PdbViewer: a historical perspective, Electrophoresis 30 (Suppl. 1) (2009) S162–S173.
[61] F. Kiefer, K. Arnold, M. Kunzli, L. Bordoli, T. Schwede, The SWISS-MODEL repository and associated resources, Nucleic Acids Res. 37 (2009) D387–D392.
[62] M.M. Mohammad, L. Movileanu, Impact of distant charge reversals within a robust beta-barrel protein pore, J. Phys. Chem. B 114 (2010) 8750–8759.
[63] E.F. Pettersen, T.D. Goddard, C.C. Huang, G.S. Couch, D.M. Greenblatt, E.C. Meng, T.E. Ferrin, UCSF chimera – a visualization system for exploratory research and analysis, J. Comput. Chem. 25 (2004) 1605–1612.